Contribution from the Department of Chemistry,
The Florida State University, Tallahassee, Florida 32306

Crystal and Molecular Structure of Dicarbonyl(2,4-pentanediimine)rhodium(I) Tetrafluoroborate, a Structure Having Extended Rhodium–Rhodium Interactions

PATRICK W. DEHAVEN and VIRGIL L. GOEDKEN*

Received August 9, 1978

The reaction of $Rh_2Cl_2(CO)_4$ with 2,4-pentanediiminium tetrafluoroborate in ethanol yields the planar Rh(I) complex $[Rh(C_5H_{10}N_2)(CO)_2]BF_4$. The metallic gold luster of this complex suggested extended Rh(I)–Rh(I) interactions. Consequently, the crystal structure was determined in order to examine the nature of these interactions and compare them with those of closely related systems. The complex crystallizes in space group $P2_1/c$ with a = 6.621 (5) Å, b = 12.309 (10) Å, c = 15.093 (10) Å, and β = 93.57 (5)°. The observed and calculated densities, 1.85 and 1.86 g/cm^3, respectively, correspond to Z = 4. The structure was solved by standard heavy-atom methods and refined by full-matrix least-squares techniques to a conventional discrepancy factor of R = 0.038 for 1722 observed reflections with $|F_o| > 3\sigma_F$. The $[Rh(C_5H_{10}N_2)(CO)_2]^+$ cations were found to form weak dimers with a Rh(I)–Rh(I) distance of 3.271 (3) Å, comparable to the distances found in a number of other Rh(I) complexes involving Rh(I)–Rh(I) extended interactions. These dimers are stacked in a columnar fashion along the a axis to form a linear Rh(I) chain, with the Rh(I)–Rh(I) distance between dimers being 3.418 (3) Å. The nonuniformity of the stacking appears to be the result of hydrogen-bonding interactions between the iminate hydrogen atoms and two of the fluorine atoms of the BF_4^- anions.

Introduction

Because of the interest in one-dimensional inorganic complexes, much work has recently been devoted to the synthesis and characterization of systems involving extended metal–metal interactions, especially linear-chain metal complexes.[1] Many of these studies have centered on the square-planar d^8 complexes of Pt(II),[2-4] especially the partially oxidized tetracyanoplatinate complexes and, to a lesser extent, complexes of Ir(I).[5,6] However, the properties of the analogous Rh(I) complexes have not been as widely explored. A few Rh(I) complexes with extended metal–metal interactions have been characterized, the best known of these being $Rh_2Cl_2(CO)_4$ with a Rh–Rh distance of 3.31 Å[10] and $Rh(acac)(CO)_2$ with a Rh–Rh distance of 3.26 Å.[8] Recently we determined the crystal structure of a binuclear Rh(I) complex, II, of the macrocyclic ligand I and a similar binuclear Rh(I) complex

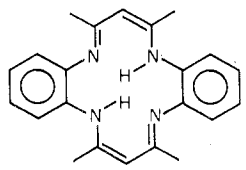

I

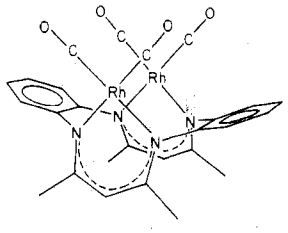

II

of I which had been protonated at the γ carbon of the six-membered ring.[7] The cations of the latter complex are located near a crystallographic inversion center producing four-atom chains comprised of two $[Rh_2(C_{22}H_{23}N_4)(CO)_4]^+$ units. The Rh(I)–Rh(I) distances in these complexes vary from 3.057 to 3.268 Å. Because the propensity for the formation of extended Rh–Rh interactions appeared to increase with protonation of the 2,4-pentanediimine chelate of the macrocyclic ligand, we have synthesized and structurally characterized a Rh(I) complex of the 2,4-pentanediimine ligand, III. This simple

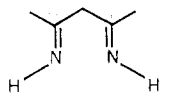

III

molecule represents the functional chelate of the protonated, complexed macrocyclic ligand I. A comparison of the structure of the Rh(I) complex of III with the structures of I permits a more full evaluation of the steric constraints inherent in the macrocyclic structures and their effects. Comparison of the Rh(I) complex of III with other Rh(I) complexes exhibiting tendencies toward solid-state interactions allows some assessment of the role of donor atom and charge of the complex on this phenomenon.

Experimental Section

The starting material, $Rh_2Cl_2(CO)_4$, was prepared by the method of McCleverty and Wilkinson.[12] Spectrograde solvents (CH_3CN, C_2H_5OH) were used for the synthesis, recrystallization, and spectral measurements. Elemental analyses were performed by Galbraith Laboratories, Knoxville, Tenn.

Infrared spectra were obtained using a Perkin-Elmer 521 grating infrared spectrophotometer in the range 4000–650 cm^{-1}. Absorption spectra were measured using a Cary 14 spectrophotometer with 1.00-cm cells and acetonitrile solutions. Solid-state spectra were obtained from hexachlorobutadiene mulls between NaCl plates.

Syntheses. $[Rh(C_5H_{10}N_2)(CO)_2]BF_4$. An ethanol solution containing 0.161 g of 2,4-pentanediiminium tetrafluoroborate (prepared by the method of McGeichin[13]) was added to a solution of 0.389 g of $Rh_2Cl_2(CO)_4$ in 3 mL of ethanol at room temperature. At high concentrations, the product precipitates immediately, forming an intensely colored blue gel. If crystal growth is slow or if the solution is allowed to stand, large needlelike crystals with a gold, metallic luster are formed (deep blue-black when crushed). The product was filtered (this should be done within 1 h of the reaction; otherwise significant decomposition occurs, resulting from hydrolysis due to the hydrochloric acid generated during the reaction), washed with a 1:1 (v/v) ethanol–diethyl ether solution, and dried in vacuo. The product was recrystallized from hot, concentrated ethanol solution. The yield was 50%. Anal. Calcd: C, 29.5; H, 2.95; N, 9.36. Found: C, 29.0; H, 3.01; N, 9.25.

Details of the X-ray Structure Determination. Crystal Examination and Data Collection. A large (0.4 × 0.2 × 0.3 mm^3) crystal of $[Rh(C_5H_{10}N_2)(CO)_2]BF_4$ in the shape of an irregular hexagon was mounted on a glass fiber. Preliminary precession photographs indicated $2/m$ (monoclinic) symmetry. The crystal was then transferred to a Hilger & Watts Y290 diffractometer for the determination of lattice constants and intensity data collection. Accurate lattice constants were obtained by a least-squares fit[14] to the $\pm 2\theta$ values of 12 independent reflections with 2θ limits $16° < 2\theta < 34°$. A listing of these lattice constants along with other pertinent cell data is given in Table I.

Intensity data were collected using Zr-filtered Mo Kα radiation. Within a sphere of $2\theta < 50°$ all data in the hkl and $hk\bar{l}$ octants were collected with a θ–2θ step-scan technique. The scan width was 1.2° (2θ) with a increment of $\Delta 2\theta = 0.04°$. Stationary-crystal, stationary-counter backgrounds were measured for 15 s at the 2θ extremes of each scan. A total of 2045 independent nonzero intensities were measured within the limits of $0 < (\sin\theta)/\lambda < 0.595$ Å^{-1}. As a check on electronic and crystal stability, the intensities of three standard

0020-1669/79/1318-0827$01.00/0

Table I. Crystal Data for $[Rh(C_5H_{10}N_2)(CO)_2]BF_4$

formula wt	342.90
space group	$P2_1/c$
a, Å	6.621 (5)[a]
b, Å	12.309 (10)
c, Å	15.093 (10)
β, deg	93.57 (5)
V, Å^3	1227.7
no. of reflections used to detn cell constants	12
2θ limits, deg	$16 \leq 2\theta \leq 34$
Z	4
μ, cm^{-1}	14.01
d_{calcd}, g/cm^3	1.86
d_{exptl}, g/cm^3	1.85 (3)

[a] In this and succeeding tables, estimated standard deviations are given in parentheses for the least significant figures.

reflections were remeasured after every 100 reflections. These standards were not observed to vary significantly throughout the entire data collection period. The intensity data (I) were corrected for Lorentz and polarization effects, and equivalent reflections were averaged; however, no corrections were made for absorption. The estimated variance in each intensity was calculated by $\sigma_I^2 = C_T + (C_{B1} + C_{B2}) + k^2(C_T + C_{B1} + C_{B2})^2$, where C_T represents the peak scan counts, C_{B1} and C_{B2} represent the background counts, and the factor k (=0.05) represents an estimate of nonstatistical errors. The intensity data were converted to relative structure factors (F_o) and estimated errors (σ_F) by $F = (I/Lp)^{1/2}$ and $\sigma_F = [(I + \sigma I)/Lp]^{1/2} - F$, with Lp = Lorentz and polarization factors. A total of 1722 reflections with $|F_o| > 3\sigma_F$ were used in the subsequent structure analysis and refinement.

Solution and Refinement of the Structure. Inspection of the data revealed the following systematic absences: $h0l$, $l = 2n + 1$, and $0k0$, $k = 2n + 1$. On the basis of these absences, the space group was uniquely determined to be $P2_1/c$. The structure was solved by standard heavy-atom methods and refined by full-matrix least-squares techniques.[15,16] The rhodium atom position was obtained from an analysis of a three-dimensional Patterson function. Two cycles of isotropic refinement of the rhodium led to an unweighted R of 38%. The positions of the remaining nonhydrogen atoms were obtained by successive structure factor and electron density map calculations. Least-squares refinement using anisotropic thermal parameters for the rhodium and isotropic thermal parameters for the remaining atoms reduced the discrepancy indices to 0.148 and 0.166 for R_1 and R_2,[17] respectively. Approximate positions for the methylene and iminato hydrogens were calculated from the carbon and nitrogen positions assuming typical C–H (0.95 Å) and N–H (1.01 Å) distances as well as idealized geometry. The positions of the methyl hydrogens were obtained by analysis of a difference Fourier map and then fitted by least squares to idealized distances and geometries. Two final cycles of refinement, with all hydrogen atoms included as fixed contributions, resulted in $R_1 = 0.038$ and $R_2 = 0.043$ for 1722 observed reflections ($|F_o| > 3\sigma_F$). A final difference map had a maximum electron density of 0.7 e/Å^3 in the vicinity of the rhodium atom.

The final positional and thermal parameters are listed in Table II. Bond distances and angles are given in Tables III and IV, respectively. A listing of observed and calculated structure factor amplitudes as well as the hydrogen atom positions is available as supplementary material.

Results and Discussion

Physical Properties of $[Rh(C_5H_{10}N_2)(CO)_2]BF_4$. Crystals of $[Rh(C_5H_{10}N_2)(CO)_2]BF_4$ grow as long needles and are extremely pleochroic. Very small crystals appear virtually colorless when viewed normal to the needle axis but take on an intense blue-black color when viewed down the needle axis. Larger crystals and bulk samples exhibit a gold, metallic luster. The compound dissolves readily in most polar organic solvents to yield yellow solutions. If the solvents are wet, hydrolysis of the 2,4-pentanediimine ligand slowly occurs resulting in the formation of the 2,4-pentanedionato complex $Rh(acac)(CO)_2$. The ease with which the complexes dissolve and the accompanying color changes indicate that the metal–metal

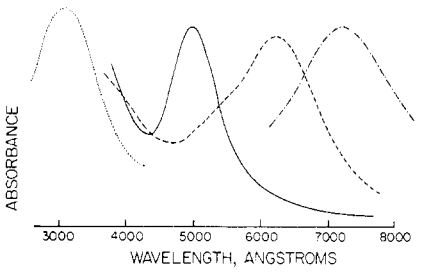

Figure 1. Spectra of four $Rh^IN_2(CO)_2$ complexes illustrating the effect of various degrees of aggregation on the visible region of the spectrum. Key: monomeric $[Rh(C_5H_{10}N_2)(CO)_2]BF_4$, acetonitrile solution (···); $Rh_2(C_{22}H_{22}N_4)(CO)_4$, II, acetonitrile solution (—); $[Rh_2(C_{22}H_{23}N_4)(CO)_4]_2(ClO_4)_2$, a tetrameric Rh(I) chain in the solid state (- - -); $[Rh(C_5H_{10}N_2)(CO)_2]_n(BF_4)_n$, extended Rh(I) interactions in the solid state (-·-).

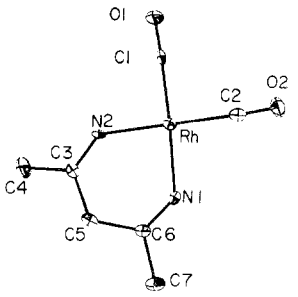

Figure 2. Structure of the $[Rh(C_5H_{10}N_2)(CO)_2]^+$ cation with the atom labeling scheme. Thermal ellipsoids are drawn at the 50% probability level; hydrogen atoms have been omitted.

interactions, while sufficient to produce marked changes in the spectral characteristics, are easily overcome by the modest solvation energies of solvents such as acetonitrile and ethanol.

The infrared spectrum of $[Rh(C_5H_{10}N_2)(CO)_2]BF_4$ exhibits two strong carbonyl absorptions at 2040 and 2090 cm^{-1} shifted only slightly from those of $Rh_2Cl_2(CO)_4$. The imine stretching frequency appears as a very strong singlet at 1670 cm^{-1}, indicating little π back-bonding into the π^* imine orbital.

Solutions of the complex are monomeric and pale yellow; they display no tendency toward aggregation via Rh–Rh interactions as has been observed for Rh(I) complexes of the phenyl isocyanide ligand.[11] Acetonitrile solutions of the complex have an intense absorption at 316 nm. This absorption undergoes a large red shift, to 725 nm, in the solid state. Figure 1 illustrates the shift in the absorption spectra as a function of the number of interacting Rh(I) atoms for a number of complexes having 2,4-pentanediimine or 2,4-pentanediiminato chelates. The values for the absorption maximum for the binuclear macrocyclic reference compound, II, and its protonated (at the γ carbon) derivative which exists as a four-atom Rh(I) chain in the solid state fall midway between the limiting values for the monomeric and extended interactions of the 2,4-pentanediimine ligand. Complex II has an absorption maximum at 405 nm (both in solution and in the solid state) whereas the four-atom cluster has its maximum at 617 nm. Gray and co-workers have presented a theoretical explanation to account for red shifts as a function of the degree of polymerization of Rh(I) complexes in solution.[19]

Description of the Structure. The Cation. The molecular structure of $[Rh(C_5H_{10}N_2)(CO)_2]^+$, as illustrated in Figure 2, consists of the Rh(I) cation coordinated to two carbon monoxide molecules and a neutral 2,4-pentanediimine chelate. As expected, the rhodium sits squarely in the carbon–nitrogen plane, the out-of-plane displacement (0.02 Å) being within the average deviation of the C1–C2–N1–N2 least-squares plane. The average Rh–C(CO) distance is 1.872 (6) Å and the average Rh–N distance is 2.041 (4) Å. These distances are

Table II. Positional and Thermal Parameters for the Atoms of $[Rh(C_5H_{10}N_2)(CO)_2]BF_4$

atom	x^a	y	z	$B_{11}{}^b$	B_{22}	B_{33}	B_{12}	B_{13}	B_{23}
Rh	0.24349 (7)	0.01767 (3)	−0.00629 (2)	21.8 (2)	5.95 (3)	3.54 (2)	−0.27 (5)	−0.38 (3)	−0.39 (2)
F1	0.0366 (7)	−0.2396 (4)	0.1486 (3)	42.0 (2)	15.6 (5)	8.8 (3)	6.8 (7)	−2.8 (5)	3.7 (3)
F2	0.2166 (10)	−0.3870 (4)	0.1310 (4)	88.0 (3)	9.3 (4)	13.5 (4)	−0.6 (8)	3.1 (8)	−2.1 (3)
F3	0.1887 (8)	−0.3242 (4)	0.2647 (3)	70.0 (2)	18.0 (6)	7.2 (2)	1.1 (9)	−6.2 (6)	4.6 (3)
F4	0.3693 (8)	−0.2325 (4)	0.1671 (4)	46.0 (2)	11.7 (4)	12.8 (4)	−4.0 (7)	−4.6 (6)	3.5 (3)
O1	0.2486 (8)	0.0605 (4)	−0.2006 (2)	49.0 (2)	9.5 (4)	3.8 (2)	1.1 (6)	−0.1 (4)	0.2 (2)
O2	0.3069 (8)	−0.2180 (3)	−0.0420 (3)	41.0 (2)	6.8 (3)	6.8 (2)	0.4 (6)	2.8 (5)	−1.2 (2)
N1	0.2573 (8)	−0.0012 (3)	0.1286 (3)	20.0 (2)	6.5 (4)	4.3 (2)	0.0 (5)	−0.5 (4)	0.4 (2)
N2	0.1940 (8)	0.1783 (4)	0.0162 (3)	28.8 (16)	6.3 (3)	3.9 (2)	0.5 (5)	−1.5 (4)	−0.3 (2)
C1	0.2431 (9)	0.0427 (4)	−0.1281 (3)	24.0 (2)	6.2 (4)	4.5 (2)	0.6 (6)	0.1 (4)	−0.5 (2)
C2	0.2863 (9)	−0.1309 (5)	−0.0276 (3)	21.0 (2)	7.4 (5)	4.4 (2)	−0.7 (6)	1.2 (4)	−0.6 (2)
C3	0.2143 (9)	0.2348 (4)	0.0860 (3)	28.0 (2)	6.3 (4)	5.2 (3)	−1.4 (6)	−0.8 (5)	−0.6 (2)
C4	0.1687 (16)	0.3520 (6)	0.0849 (5)	78.0 (4)	6.5 (5)	8.4 (4)	4.3 (12)	−3.7 (10)	−1.5 (4)
C5	0.2747 (10)	0.1872 (5)	0.1743 (3)	35.0 (2)	8.4 (5)	4.1 (2)	−1.5 (8)	0.2 (5)	−1.1 (2)
C6	0.2684 (9)	0.0693 (5)	0.1912 (3)	16.0 (2)	9.4 (5)	4.1 (2)	−0.2 (6)	0.0 (4)	−0.3 (2)
C7	0.2856 (12)	0.0341 (6)	0.2859 (4)	39.0 (3)	11.1 (6)	4.3 (2)	1.2 (9)	1.0 (6)	0.5 (3)
B	0.2019 (14)	−0.2937 (6)	0.1796 (5)	36.0 (3)	7.7 (6)	5.7 (3)	0.9 (10)	−1.4 (7)	1.7 (3)

[a] Estimated standard deviations in the least significant figure(s) are given in parentheses in this and all subsequent tables. [b] The form of the anisotropic thermal ellipsoid is $\exp[-(B_{11}h^2 + B_{22}k^2 + B_{33}l^2 + 2B_{12}hk + 2B_{13}hl + 2B_{23}kl)]$. The quantities given in the table are the thermal coefficients $\times 10^3$.

Table III. Interatomic Distances (A) for $[Rh(C_5H_{10}N_4)(CO)_2]BF_4$

Rh-Rh[a]	3.271 (3)	C3-C5	1.487 (7)
Rh-Rh[b]	3.418 (3)	C5-C6	1.474 (8)
Rh-C1	1.864 (5)	C6-N1	1.282 (7)
Rh-C2	1.881 (6)	C6-C7	1.492 (7)
Rh-N1	2.045 (4)	B-F1	1.340 (8)
Rh-N2	2.036 (5)	B-F2	1.369 (9)
C1-O1	1.119 (6)	B-F3	1.347 (8)
C2-O2	1.104 (7)	B-F4	1.363 (10)
C3-N2	1.263 (6)	N1-F4	2.989 (7)
C3-C4	1.474 (9)	N2-F1[a]	2.935 (6)

[a] Position related to that of reference molecule by $(x, y, z) \rightarrow (\bar{x}, \bar{y}, \bar{z})$. [b] Position related to that of reference molecule by $(x, y, z) \rightarrow (1 - x, \bar{y}, \bar{z})$.

Table IV. Interatomic Angles (deg) for $[Rh(C_5H_{10}N_2)(CO)_2]BF_4$

Rh[a]-Rh-Rh[b]	163.68 (3)	N2-C3-C5	122.6 (5)
N1-Rh-N2	86.7 (2)	C4-C3-C5	116.1 (5)
N1-Rh-C1	176.1 (2)	C3-C5-C6	122.3 (4)
N1-Rh-C2	93.5 (2)	C5-C6-C7	116.8 (5)
N2-Rh-C1	90.7 (2)	C5-C6-N1	122.6 (5)
N2-Rh-C2	179.4 (2)	C7-C6-N1	120.5 (5)
C1-Rh-C2	89.0 (2)	F1-B-F2	108.3 (6)
Rh-N1-C6	130.8 (4)	F1-B-F3	111.8 (7)
Rh-N2-C3	131.6 (4)	F1-B-F4	109.3 (6)
Rh-C1-O1	177.4 (5)	F2-B-F3	106.7 (6)
Rh-C2-O2	177.9 (6)	F2-B-F4	107.7 (7)
N2-C3-C4	121.2 (6)	F3-B-F4	112.8 (6)

[a] Position related to that of reference molecule by $(x, y, z) \rightarrow (\bar{x}, \bar{y}, \bar{z})$. [b] Position related to that of reference molecule by $(x, y, z) \rightarrow (1 - x, \bar{y}, \bar{z})$.

within the range expected for Rh(I) and do not differ appreciably from the Rh(I)–C and Rh(I)–N distances observed in the macrocyclic complexes containing 2,4-pentanediimine and 2,4-pentanediiminato ligand fragments.[7] The average imine bond length is 1.275 (7) Å and indicates little, if any, back-bonding by rhodium to the π^* imine orbitals, in agreement with the IR results. One of the more interesting aspects associated with the 2,4-pentanediimine ligand is the C3–C5–C6 angle, 122.3 (4)°, which is much larger than that expected for a methylene carbon having sp^3 hybridization. This angle is equal, within experimental error, to that found in the sp^2 carbons of N=C–C, 122.6 (5)°. It is likely that this angle is the result of constraints placed on the 2,4-pentanediimine ligand, i.e., the bite size required for normal Rh(I) square-planar coordination geometry, sp^2 hybridization for the imine carbon atoms, and the requirement of coplanarity within

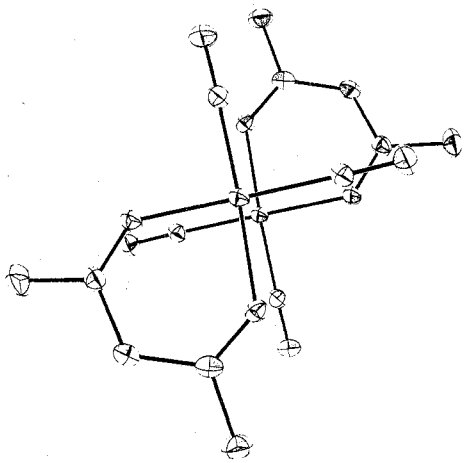

Figure 3. The two closest interacting $[Rh(C_5H_{10}N_2)(CO)_2]^+$ cations, viewed perpendicular to the coordination plane, to illustrate the slight dislocation of the donor atoms relative to one another.

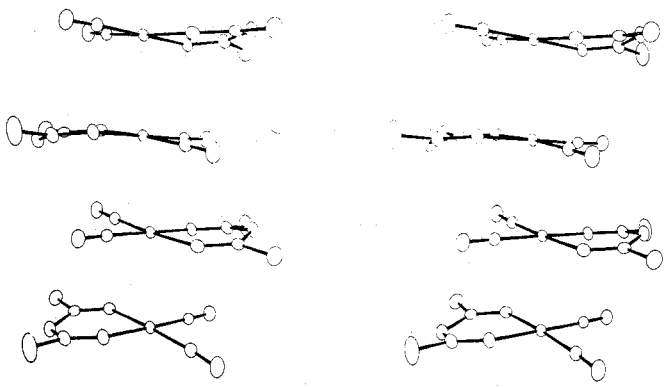

Figure 4. Stereoview of stacking arrangement illustrating extended Rh(I) interactions.

the ligand in order to maximize double-bond overlap (it should be noted that the methylene carbon is displaced only 0.17 Å from the plane defined by the two imine groups). However, it appears that these constraints can vary in their magnitude and effect. For example, there is a notable increase in the out-of-plane displacement (~0.7 Å) and corresponding reduction in the methylene carbon angle (116 (2)°) for the 2,4-pentanediimine moiety in $[Rh_2(C_{22}H_{23}N_4)(CO)_4]ClO_4$,[7] while a Co(II) macrocyclic complex[18] which also contains the 2,4-pentanediimine fragment has an angle (121.9 (7)°) and

Table V. Comparison of Rh(I)-Rh(I) Distances in Stacked or Binuclear Rh(I) Complexes

complex	Rh(I)-Rh(I) dist, Å	comments	ref
$[Rh(acac)(CO)_2]_n$	3.26 (1), 3.27 (1)	extended Rh(I) Rh(I)-Rh(I) interactions; columnar stacking	8
$[Rh(CO)_2(CF_3CO)_2CH]_n$	3.34 (1)	extended Rh(I)-Rh(I) interactions; columnar stacking	8
$[(CO)_2RhNCOC_6H_5]_2$	3.347 (5)	Rh(I) dimers stacked in stepwise fashion	9
$[Rh(C_5H_{10}N_2)(CO)_2]BF_4$	3.271 (3), 3.418 (3)	weak Rh(I) dimers stacked in columnar fashion	this work
$Rh_2Cl_2(CO)_4$	3.31	extended Rh(I)-Rh(I) interactions between dimers to form infinite Rh(I)-Cl-Rh(I) chains	10
$[Rh_2(C_{22}H_{23}N_4)(CO)_4]^+$	3.057 (3), 3.268 (4)	four-atom Rh(I) chain	7
$Rh_2(C_{22}H_{22}N_4)(CO)_4$	3.0860 (5)	binuclear Rh(I)	7
$[Rh_2(CNPh_8)](BPh_4)_2$	3.193 (0)	binuclear Rh(I)	11

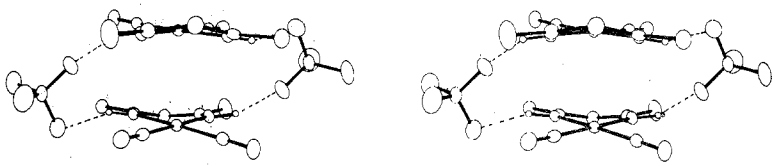

Figure 5. Stereoview of the weak Rh(I) dimers illustrating the hydrogen bonding interactions between the BF_4^- anions and the N–H hydrogen atoms, which are presumed to be responsible for the formation of a dimeric species as opposed to a uniform stacking arrangement.

out-of-plane displacement (0.05 Å) similar to that found in this study.

Due to the size of the C3–C5–C6 angle, one would expect considerable driving force toward the loss of a proton, producing sp^2 carbon and yielding the 2,4-pentanediiminato ligand. However, attempts to isolate the molecular complex by deprotonation of the ligand have been unsuccessful to date; instead some complex decomposition occurs, and in the presence of chloride a complex which appears to be $Rh(C_5H_{10}N_2)(CO)_2Rh(CO)_2Cl_2$ results. If the deprotonated species is formed in solution, it appears to have a lesser tendency to undergo dimerization or oligomerization reactions than the cationic species.

Nearest-Neighbor Interactions. As illustrated in Figure 3, the $[Rh(C_5H_{10}N_2)(CO)_2]^+$ cations are located near a crystallographic inversion center, producing a weak dimer with a Rh(I)–Rh(I) distance of 3.271 (3) Å. These dimers are stacked along the *a* axis in a linear fashion, with a relatively long Rh(I)–Rh(I) distance of 3.418 (3) Å between dimers. A stereoview of this stacking arrangement is given in Figure 4. Despite the relatively long distance between dimers, this interaction is apparently responsible for the cations crystallizing in the observed stacked manner and accounts for the metallic gold luster of the crystals and the pronounced differences between the solution and solid-state spectra. It is unlikely that a simple dimer alone would be responsible for the relatively large red shift of the bands.

The Rh(I)–Rh(I) distance of 3.271 (3) Å is comparable to that found in a number of Rh(I) complexes involving extended metal–metal interactions. A comparison of these complexes is given in Table V. Inspection of this table reveals a wide variety of packing arrangements as well as a reasonably broad range of Rh–Rh distances (3.057–3.418 Å), though all distances are too long to infer single-bond formation. It should be noted that with the exception of $Rh_2(C_{22}H_{22}N_4)(CO)_4$ and $[Rh_2(C_{22}H_{23}N_4)(CO)_4]^+$, in which the macrocyclic ligand serves as a bridging unit between two Rh(I) centers, none of the Rh(I)–Rh(I) interactions for the complexes listed involve bridging ligands. Also, the variety of structures found in Table V implies that the choice of ligand can affect not only the magnitude of the metal–metal interactions but also profoundly influences the stacking arrangement, which itself can affect metallic behavior. This has important implications in the directed synthesis of d^8 metal complexes exhibiting one-dimensional metal characteristics. For example, one electron band theory would predict that $Rh(acac)(CO)_2$,[8] with its equally spaced linear chain of Rh(I) cations, should be more likely to exhibit metallic behavior than the structure under consideration, which consists of stacked dimers.

It is reasonable to ask why the structure of $[Rh(C_5H_{10}N_2)(CO)_2]BF_4$ consists of stacked dimers, rather than a uniform stacking arrangement. Examination of the packing of the BF_4^- anions and the cations, as shown in the stereopacking diagram of Figure 5, and inspection of the nearest contact distances within the structure reveal that hydrogen-bonding interactions exist between the N–H hydrogens and two of the fluorine atoms of the BF_4^- anions. Although such interactions are undoubtedly weak, as evidenced by the average N–F distance of 2.962 (7) Å, and are probably no more than 2–3 kcal/mol, the accumulative effect of four such interactions per dimer unit would total 8–12 kcal/mol and account for the observed dimer units. Consistent with this is the observation of a relatively well-defined BF_4^- geometry (the BF_4^- anion in the absence of hydrogen-bonding interactions or large lattice forces has an unfortunate proclivity for high thermal motions and/or disorder).

Acknowledgment. This research was supported in part by the National Institutes of Health, Grant No. HL 14827.

Registry No. $[Rh(C_5H_{10}N_2)(CO)_2]BF_4$, 68423-69-8; $Rh_2Cl_2(CO)_4$, 14523-22-9.

Supplementary Material Available: A listing of observed and calculated structure factor amplitudes as well as the calculated hydrogen atoms positions (9 pages). Ordering information is given on any current masthead page.

References and Notes

(1) For reviews see: (a) *ACS Symp. Ser.*, **No. 5** (1974); (b) J. S. Miller and A. J. Epstein, *Prog. Inorg. Chem.*, **20**, 1 (1974).
(2) A. H. Reis, Jr., S. W. Peterson, and S. C. Lin. *J. Am. Chem. Soc.* **98**, 7839 (1976), and references cited therein.
(3) K. Krogman, *Z. Anorg. Allg. Chem.*, **358**, 97 (1968).
(4) J. M. Williams, M. Iwata, S. W. Peterson, K. A. Leslie, and H. J. Guggenheim, *Phys. Rev. Lett.*, **34**, 1653 (1974).
(5) A. H. Reis, V. S. Hagley, and S. W. Peterson, *J. Am. Chem. Soc.*, **99**, 4184 (1977).
(6) K. Krogman, W. Binder, and H. D. Hausen, *Angew. Chem., Int. Ed. Engl.*, **7**, 812 (1968).
(7) G. C. Gordon, P. W. DeHaven, M. C. Weiss, and V. L. Goedken, *J. Am. Chem. Soc.*, **100**, 1003 (1978).
(8) N. A. Bailey, E. Coates, G. B. Robertson, F. Bonati, and R. Ugo, *Chem. Commun.*, 1041 (1967).
(9) R. J. Doedens, *Inorg. Chem.*, **17**, 1315 (1978).

(10) L. F. Dahl, C. Martell, and D. L. Wampler, *J. Am. Chem. Soc.*, **83**, 1761 (1961).
(11) K. R. Mann, N. S. Lewis, R. M. Williams, H. B. Gray, and J. G. Gordon II, *Inorg. Chem.*, **17**, 828 (1978).
(12) J. A. McCleverty and G. W. Wilkinson, *Inorg. Synth.*, **8**, 211 (1966).
(13) S. G. McGeichin, *Can. J. Chem.*, **46**, 1903 (1968).
(14) W. R. Busing and H. A. Levy, *Acta Crystallogr.*, **22**, 457 (1967).
(15) Computations were performed by a CDC CYBER 73 computer with the aid of the following programs: Zalkin's FORDAP Fourier program, Busing and Levy's ORFFE function and error program, and Ibers' NUCLS least-squares program. Plots of the structures were drawn with the aid of C. K. Johnson's ORTEP.
(16) Heavy-atom scattering factors were taken from D. T. Cromer and J. B. Mann, *Acta Crystallogr., Sect. A*, **24**, 321 (1968). Hydrogen atom scattering factors were taken from "International Tables for X-Ray Crystallography", Vol. III, Kynoch Press, Birmingham, England, 1962. Anomalous scattering corrections were applied to the rhodium and fluorine atoms and were taken from D. T. Cromer, *Acta Crystallogr.*, **18**, 17 (1965).
(17) The discrepancy indices are given by $R_1 = \sum||F_o| - |F_c||/\sum|F_o|$ and $R_2 = [(\sum w|F_o| - |F_c|)^2/\sum w|F_o|^2]^{1/2}$.
(18) G. W. Roberts, S. C. Cummings, and J. A. Cunningham, *Inorg. Chem.*, **15**, 2503 (1976).
(19) K. R. Mann, J. G. Gordon II, and H. B. Gray, *J. Am. Chem. Soc.*, **97**, 3553 (1975).

Contribution from the Departments of Chemistry, Washington State University, Pullman, Washington 99164, and California Institute of Technology, Pasadena, California 91125

Molecular Structure and Magnetic Properties of the Chloro-Bridged Dimer Chloro[hydrotris(1-pyrazolyl)borato]copper(II). Observation of a Ferromagnetic Ground State

STEPHANIE G. N. ROUNDHILL,[1a] D. MAX ROUNDHILL,*[1a] DARREL R. BLOOMQUIST,[1a] CHRISTOPHER LANDEE,[1a] ROGER D. WILLETT,[1a] DAVID M. DOOLEY,[1b] and HARRY B. GRAY[1b]

Received August 4, 1978

The complexes $\{CuCl[HB(1\text{-}pz)_3]\}_2$ and $CoCl[HB(1\text{-}pz)_3]$ have been prepared. The crystal structure of the copper(II) compound has been solved and the magnetic susceptibility measured. The compound belongs to the $P2_1/n$ space group with $Z = 2$, $a = 13.1440$ (15) Å, $b = 13.247$ (3) Å, $c = 7.467$ (13) Å, and $\beta = 96.073$ (14)°. The centrosymmetric structure has symmetric chloro bridges between the coppers leading to a distorted five-coordinate geometry about these metal centers. The geometry about each copper approximates that of a distorted square pyramid. The bridging chlorides and two ligand nitrogen atoms form the base of the pyramid, and the third ligand nitrogen occupies the axial site. The planar Cu_2Cl_2 bridge has Cu–Cl distances of 2.306 (2) and 2.316 (2) Å and a Cu–Cl–Cu angle of 94.51 (7)°. The electronic and EPR spectra are compatible with such a structure. The susceptibility data down to a temperature of 2 K show the presence of a ferromagnetically coupled ground state ($2J/k = 48.6$°) for the dimer. The data have been fitted in accord with a model of Heisenberg dimers with Ising-like coupling to adjacent dimers. The complex $CoCl[HB(1\text{-}pz)_3]$ shows an electronic spectrum in solution suggestive of a pseudotetrahedral geometry about Co(II).

Salts of the hydrotris(1-pyrazolyl)borate anion have been prepared by Trofimenko.[2] The anion is a very useful anionic tridentate chelating ligand which forms complexes with first-row transition-metal ions. The ligand is particularly amenable for coordination in the three facial positions of an octahedral complex, and a series of such complexes, $M[HB(1\text{-}pz)_3]_2$, has been prepared.[3] Less effort has been devoted to using the ligand for imposing a distorted four- or five-coordinate geometry about these metal ions, but this chelate ligand can potentially be used to create such a geometric environment about the metal ion. We now report our structural, spectroscopic, and magnetic results obtained with the compound $\{CuCl[HB(1\text{-}pz)_3]\}_2$.

Previous structural work on hydrotris(1-pyrazolyl)borato complexes of copper has centered mainly on the copper(I) compounds. The compound $\{Cu[HB(1\text{-}pz)_3]\}_2$ is bridged by the third pyrazolyl nitrogen from each hydrotris(1-pyrazolyl)borato ligand, and the geometry about the central copper(I) ion can be roughly described as a distorted tetrahedron.[4] A crystal structure study of the carbonyl complex $Cu(CO)[HB(1\text{-}pz)_3]$ shows the compound to be monomeric with molecules having both precise and distorted C_{3v} symmetries about copper(I) in the unit cell.[5] More recently the structure of the copper(I) complex $K[Cu(p\text{-}NO_2C_6H_4S)[HB(3,5\text{-}Me_2(1\text{-}pz))_3]_2\cdot(CH_3)_2CO$ has been reported, and this too has a distorted tetrahedral geometry about the metal center.[6] It should be possible, therefore, to prepare hydrotris(1-pyrazolyl)borato complexes of divalent copper with a single monodentate ligand such as halide coordinated to the metal, thereby placing the metal ion in an unsymmetrical environment.

Treating anhydrous cupric chloride with an equimolar quantity of sodium hydrotris(1-pyrazolyl)borate in an ethanol or acetonitrile solvent system leads to the isolation in good yield of a copper(II) complex having the stoichiometry $CuCl[HB(1\text{-}pz)_3]$ (eq 1). The complex is not monomeric but is

$$2CuCl_2 + 2Na[HB(1\text{-}pz)_3] \rightarrow \{CuCl[HB(1\text{-}pz)_3]\}_2 + 2NaCl \quad (1)$$

symmetrically bridged by chloro ligands between the copper ions. This geometric arrangement has been confirmed by a single-crystal X-ray structural study, and the electronic and EPR spectral data are in agreement with such a structure. Using a similar procedure it is possible to isolate the stoichiometrically analogous cobalt(II) complex $CoCl[HB(1\text{-}pz)_3]$ (eq 2). This latter compound is very unstable to ligand

$$CoCl_2 + Na[HB(1\text{-}pz)_3] \rightarrow CoCl[HB(1\text{-}pz)_3] + NaCl \quad (2)$$

disproportionation in solution, probably because of the coordination of the strong ligand field hydrotris(1-pyrazolyl)borato chelate about a pseudotetrahedral metal ion (eq 3).

$$2CoCl[HB(1\text{-}pz)_3] \rightarrow CoCl_2 + Co[HB(1\text{-}pz)_3]_2 \quad (3)$$

Experimental Section

Anhydrous cupric chloride was prepared by heating the hydrate at 100 °C for 12 h. Sodium hydrotris(1-pyrazolyl)borate was prepared by a published procedure. Electronic spectra were measured as

0020-1669/79/1318-0831$01.00/0